Observation of enhanced Rayleigh scattering produced by optical mixing in gases

J. Meyer and G. G. Albach
Department of Physics, The University of British Columbia, Vancouver, British Columbia, Canada V6T 1W5
(Received 16 January 1975; revised manuscript received 3 September 1975)

The effect of mixing two high-power ruby-laser beams in several gases has been investigated by means of light scattering. Coherently scattered light has been observed with intensities of up to three orders of magnitude, exceeding that of incoherent Rayleigh scattered light. The dependence of the effect on laser power, gas density, and refractive index is described. It is shown that for higher pressures ($\sim$ 100 Torr) a threshold power exists for the effect, and that saturation is observed with increasing pressure as well as increasing mixing beam power.

I. INTRODUCTION

Nonlinear interactions between intense electromagnetic waves and neutral gas molecules can be of significance, e.g., inside high-power gas-laser cavities and in studies of laser-produced gas breakdown. High-power laser radiation can interact strongly with the density fluctuations and thus influence, e.g., optical properties like the backscattering characteristics and electrical breakdown strength of a gas. Effects like stimulated Rayleigh scattering have been observed in gases irradiated by intense laser light.[1] Here we want to report on an effect, which will be predominant if two laser beams interact with a gas, a situation met, e.g., in gas-laser cavities. This mixing effect has previously been observed in a plasma.[2]

If one considers a classical oscillator (molecule) of polarizability α in the field of two electromagnetic waves of wave vectors $\vec{k}_1$ and $\vec{k}_2$ and frequencies ω_1 and ω_2, one can show that the nonlinear $\vec{v}\times\vec{B}$ term of the Lorentz force acting on the oscillating electron results in a second-order force of the form

$$\vec{F}_{(2)} = (\alpha/2)\vec{E}_1 \cdot \vec{E}_2 \, (\vec{k}_1 - \vec{k}_2) \times \sin[(\omega_1 - \omega_2)t - (\vec{k}_1 - \vec{k}_2)\cdot\vec{r}] \, . \quad (1)$$

$\vec{E}_{1,2}$ are the electric field amplitudes of the two incident electromagnetic waves. If the frequency difference $(\omega_1 - \omega_2)$ is very small the oscillator may be displaced significantly under the influence of this force. This situation arises, for example, when the two beams are produced by the same laser.

$\vec{F}_{(2)}$ of Eq. (1) can be derived from a potential. Setting $\omega_1 - \omega_2 = 0$, one can write for the potential energy distribution of the gas molecules

$$W_{\text{pot}} = (\alpha/2)\vec{E}_1 \cdot \vec{E}_2 \cos[\vec{k}_1 - \vec{k}_2)\cdot\vec{r}] \, . \quad (2)$$

Under the influence of this potential distribution the gas density will be modulated. By coherent light-scattering experiments of a third diagnostic beam, where the difference of incident and scattered-wave vectors matches $\vec{k}_1 - \vec{k}_2$, one can detect this modulation in that one measures the autocorrelation function of the density $\langle |n(\vec{k}_1 - \vec{k}_2)|^2\rangle$. Fig. 1 shows a diagram of the wave vectors involved. The diagnostic wave number is chosen to be double the ruby wave number. The autocorrelation function in the presence of the potential distribution of Eq. (2) can be calculated if the potential energy is very much smaller than the thermal energy of the gas molecules. Assuming in this case, that the initial Maxwellian particle distribution function is only slightly perturbed, one finds

$$\langle |n(\vec{k})|^2\rangle = N\left[1 + N\left(\frac{\alpha \vec{E}_1 \cdot \vec{E}_2}{2KT}\right)^2 \delta[\vec{k} - (\vec{k}_1 - \vec{k}_2)]\right] . \quad (3)$$

Here N is the number of molecules in the interaction volume.

If however, the potential amplitude becomes of the same order as the thermal energy then the calculation is greatly complicated. At equilibrium one expects a Maxwell-Boltzmann distribution to be established, resulting in a similar expression for $\langle |n(k)|^2\rangle$ as given by Eq. (3).

However, with laser pulses lasting a few tens of nanoseconds and intercollision times of the same order equilibrium will not be reached during the interaction time. A theory describing this situation would have to be very complicated, taking into account effects like particle trapping. It seems therefore desirable to study the effect experimentally in order to stimulate and aid theoretical investigations.

II. EXPERIMENT

The experimental arrangement is shown in Fig. 2. The mixing beams are generated by a 250-MW

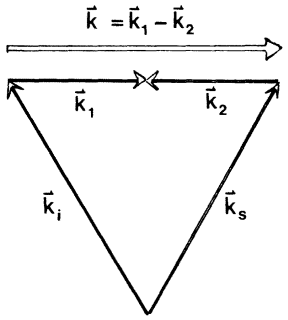

FIG. 1. Wave-vector diagram for mixing and scattering geometry. $\vec{k}_{1,2}$ are the mixed wave vectors; $\vec{k}_i$ and $\vec{k}_S$ are diagnostic and scattered wave vector, respectively.

pulsed ruby laser oscillator-amplifier combination with a spectral line width of 0.03 Å. The laser output is focused into a pinhole and then imaged into the gas vessel, to a focal diameter of 0.3 mm. Transmitted light is collimated and reflected back into the experimental-gas volume, thus providing the second beam for mixing. In the vessel a maximum power of 150 MW per beam could be achieved. A saturable dye cell (cryptocyanine in methanol) is placed in the path of the beam. This prevents formation of an active laser cavity consisting of amplifier ruby, front oscillator mirror and rear beam reflector. In addition it allows a controlled variation of light intensity in the gas vessel by changing the dye concentration.

A glass plate reflects 30% of the laser light into a third beam. After reflection through two prisms this beam is passed through an inverting telescope followed by a frequency-doubling RDP crystal. A cell containing a solution of copper sulphate in water is used to block the fundamental ruby light while passing the 4-MW second-harmonic ultraviolet beam used for diagnostics. This beam is focused into the gas vessel at an angle of 60° with respect to one mixing beam and 120° with respect to the other. To satisfy the wave-vector condition for coherent scattering, scattered light is gathered at an angle of 60° with respect to both the incident frequency-doubled beam and the first mixing beam. This light is passed through a monochromator of 0.3 Å bandwidth centered on the doubled ruby frequency and detected by a photomultiplier. Intensities of the uv diagnostic beam and the mixing ruby beams are monitored by a photomultiplier and photodiode, respectively.

The gas vessel was filled with either hydrogen, argon, nitrogen, or carbon dioxide at pressures varying from 5 to 100 torr. Over this range gas breakdown did not occur. For each shot the scattered signal was normalized to the intensity of the incident ultraviolet beam. Light baffles in the gas vessel and in the detection optics reduced stray laser light to a negligible level as evidenced by the total absence of a scattering signal with no gas in the vessel. With one or both mixing ruby beams blocked off, the normal Rayleigh scattered light

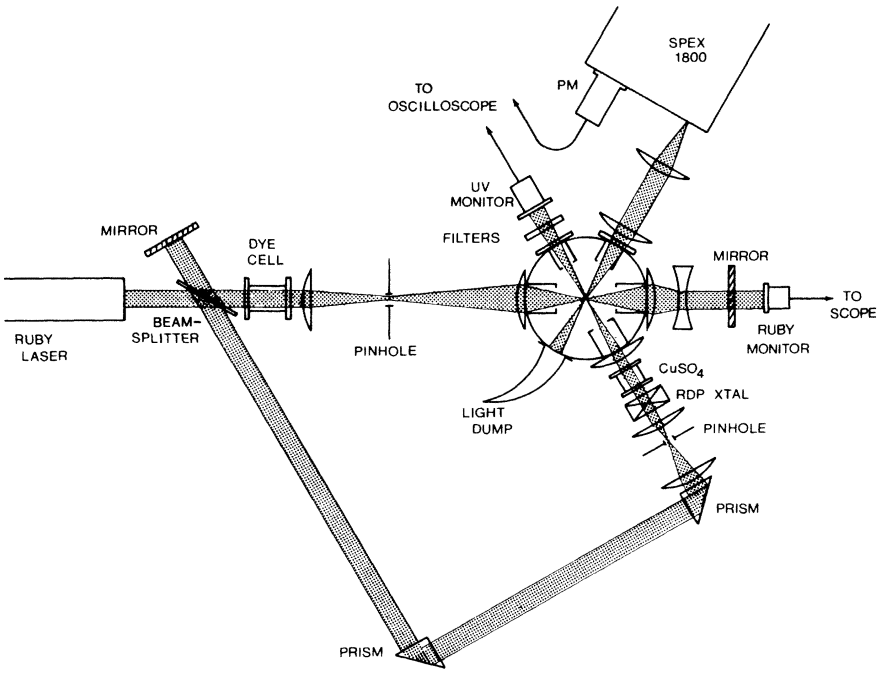

FIG. 2. Experimental arrangement.

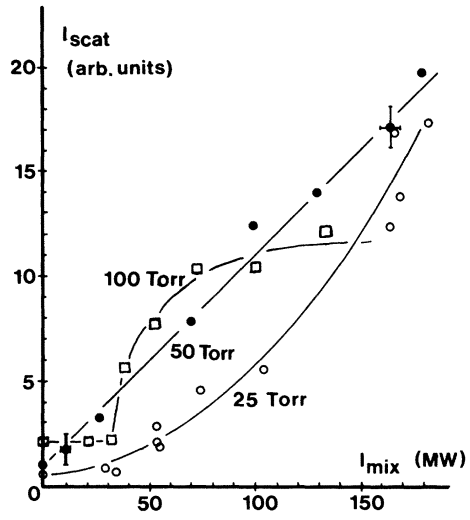

FIG. 3. Scattered-light intensity as function of mixing beam power for different pressures of hydrogen.

from the diagnostic beam could be recorded. With both mixing beams on, the enhanced scattering of the diagnostic beam was recorded.

III. RESULTS

Figure 3 shows results of experiments with hydrogen. Plotted is scattered-light intensity as function of power in one of the mixed beams for three different pressures. At zero mixing-beam power one observes the incoherent thermal Rayleigh scattering alone. As the power in the mixed ruby beams is increased, coherent scattering becomes more and more predominant. At 25 torr one observes the quadratic dependence on mixed beam power ($\propto E_1^2 E_2^2$) predicted by the simplified theoretical result of Eq. (3). At 50 torr this dependence, however, becomes linear within the experimental accuracy. At pressures of 100 torr and higher the characteristics of the effect changes. It appears that now a threshold power is needed to induce density modulations. Beyond this threshold the modulation amplitude increases more rapidly than for 50 torr but soon saturates. Similar dependencies are observed for the other investigated gases. Figure 4 shows, e.g., results observed in 100 torr carbon dioxide, for which the highest scattered intensities were observed. The existence of a threshold is clearly demonstrated. Beyond this threshold the scattered intensity rises rapidly until it reaches a value exceeding the incoherent Rayleigh scattering by nearly three orders of magnitude. At even higher mixing-beam powers the scattered intensity rapidly saturates. A second set of results is shown in Fig. 5. Here the enhancement of scattered intensity at 100 MW per mixing beam normalized to a quantity proportional to α^2 is plotted as a function of pressure for different gases. Enhancement E is defined as ratio of total

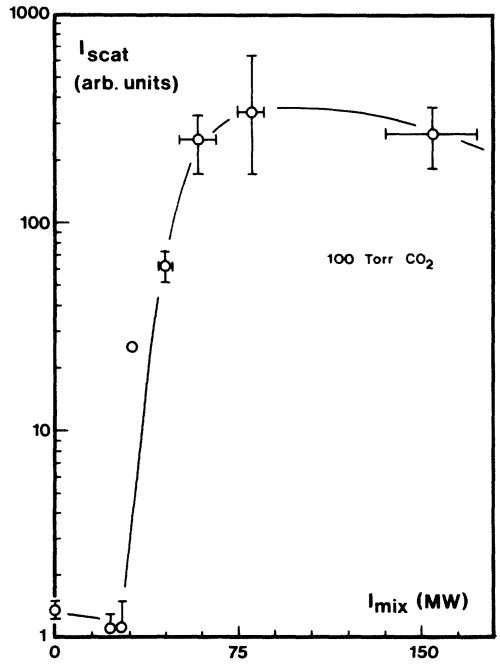

FIG. 4. Scattered-light intensity as function of mixing beam power for 100 Torr CO_2.

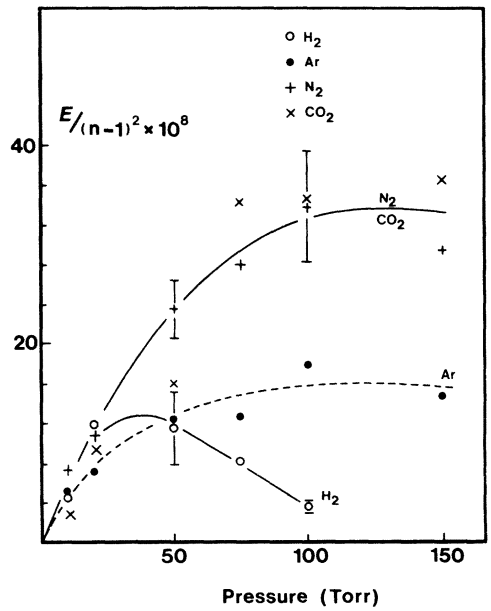

FIG. 5. Normalized enhancement of scattered-light intensity at 100 MW per mixing beam as function of pressure for different gases (n is the refractive index at standard temperature and pressure).

scattered intensity observed with mixed beams present, minus incoherent scattered intensity, observed with mixed beams blocked off, over incoherent scattered intensity. n is the index of refraction at standard pressure. For n very close to unity, the quantity $(n-1)$ is proportional to the polarizability α.

The error bars in all graphs represent the standard deviations of the mean for at least eight measurements. The magnitude of the errors are thought to be caused by shot-to-shot variation of mode structure of the laser system resulting in variation of angular intensity distribution in the interaction volume of both the mixed and diagnostic beams.

Equation (3) suggests that the results for all gases should follow the same curve and that the dependence on pressure be quadratic. Within the experimental errors this may be the case for low pressures (≤ 20 torr). For pressures of 50 torr and higher the curves, however, separate significantly and saturation of the effect is observed at higher pressures. In hydrogen the enhancement even decreases significantly with increasing pressure.

We investigated as well the angular distribution of the enhanced scattered light by varying the acceptance angle of the detection optics. The results showed that the coherently scattered light formed a beam distributed over a small solid angle equal to that of the diagnostic beam. The experiments as well indicated that the choice of the correct angle between diagnostic and mixed beams is essential, if enhanced scattering is to be observed.

IV. DISCUSSION AND CONCLUSION

The experiments demonstrate that the interaction between molecules and two laser beams may perturb the density distribution of a gas significantly. For gas pressures of 25 torr and lower, the results can be explained by a simple theory resulting in Eq. (3). For higher pressures this theory breaks down indicating, that now additional effects have to be taken into account. One may speculate that at pressures of 50 torr and higher, gas heating becomes important, resulting in smaller scattered intensities than predicted by Eq. (3). On the other hand, the observation of a threshold indicates that for pressures of 100 torr and higher some stimulated effect is produced which may be related to stimulated Rayleigh or Brillouin scattering.

ACKNOWLEDGMENT

The project has been supported by the Atomic Energy Control Board of Canada.

[1]T. A. Wiggins *et al.*, Phys. Rev. Lett. 20, 831 (1968).

[2]G. G. Albach and J. Meyer, Phys. Rev. Lett. 34, 926 (1975).

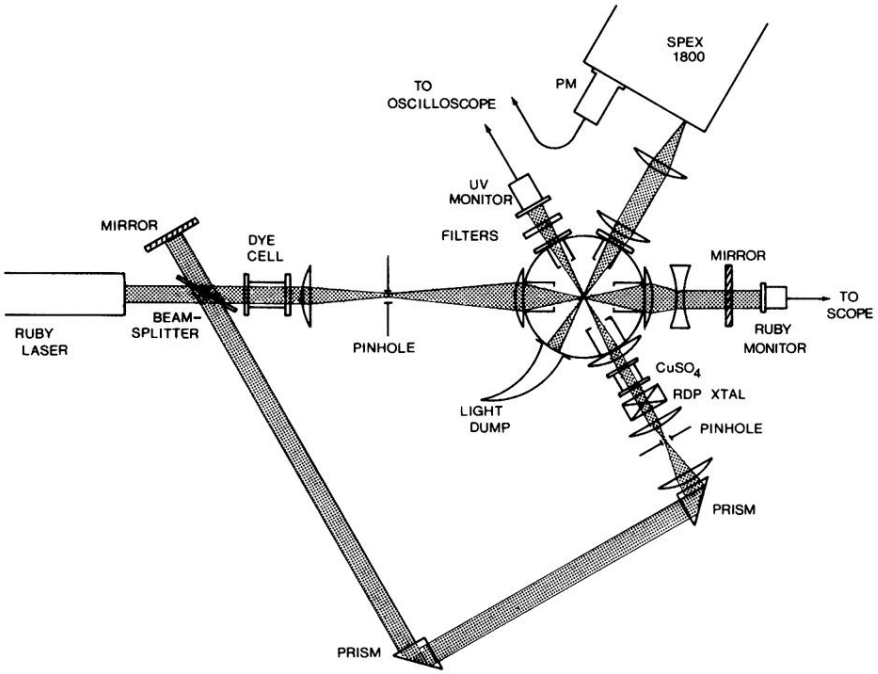

FIG. 2. Experimental arrangement.